A Comparison Between Two MPC Algorithms for Demand Charge Reduction in a Real-World Microgrid System

Yun Xue, Michael Todd, Sadrul Ula, Matthew J. Barth, and Alfredo A. Martinez-Morales

University of California - Riverside, CA 92557

***Abstract* — This paper describes an evaluation between two model predictive control (MPC) algorithms for microgrid energy management combined with solar production and battery energy storage for demand charge reduction in a real-world microgrid system. The first control algorithm is a constant threshold MPC (CT-MPC) that works well on a system with relatively stable solar generation and a well-known building load profile. CT-MPC can maintain the on-peak demand under a certain value during the entire on-peak rate period. The second control algorithm is an adjusting demand threshold MPC (ADT-MPC). ADT-MPC can better deal with unpredictable solar generation and/or changing building loads. The on-peak threshold under this algorithm is adjusted to the optimal value during the on-peak rate period. As expected, The CT-MPC algorithm performs well when coupled with accurate forecast models while the ADT-MPC algorithm excels when forecasting is more unpredictable.**

***Index Terms* — building demand, on-peak demand reduction, energy management system, microgrid, MPC, optimization.**

I. INTRODUCTION

Based on the microgrid definition by the U.S. Department of Energy Microgrid Exchange Group [1], a microgrid should have the ability to generate and distribute energy within its internal architecture, as well as being able to control different load components as a single intelligent network entity. The on-site energy generated from the microgrid system can be from renewable energy sources such as solar and wind. In 2014, renewable electricity capacity contributed 28.5% to total electricity capacity globally [2]. In 2015 Q2, solar energy represented 40% of all new electrical generation capacity in the U.S. [3]. Due to the intermittent nature of renewable sources such as solar, energy storage systems have been integrated into the architecture of microgrid systems to make them more efficient and robust. Within a microgrid system that is applied to a time-of-use (TOU) electricity rate schedule, the battery energy storage system (BESS) can be used to reduce the electricity cost by delivering energy during the on-peak rate period and storing energy (i.e. charging) during the off-peak rate period.

The goal of this study is to perform a side-by-side comparison between a constant threshold MPC (CT-MPC) algorithm and an adjusting demand threshold MPC (ADT-MPC) algorithm to determine the effectiveness of each method to lower demand charges, while maintaining a high state of charge (SOC) of the BESS during operation. This was tested on the Sustainable Integrated Grid Initiative (SIGI) microgrid system which is composed of 500 kW of solar PV generation, 1.1 MWh of Li-ion battery energy storage, and three facility buildings, which include one administrative building (1084) and two research buildings (1086 and 1200) at the College of Engineering Center for Environmental Research and Technology (CE-CERT), University of California, Riverside. The integration of a BESS within a microgrid architecture that includes renewable generation provides a dual benefit: 1) it makes the microgrid system more controllable, reliable and robust by managing the intermittent nature of renewable sources, and 2) adds economic value to the operation of the microgrid by implementing a variety of energy management strategies, including the reduction of demand charges under a time-of-use (TOU) electricity rate schedule. UCR's microgrid is located in the Riverside Public Utilities (RPU) territory in Southern California. The TOU rate schedule costs are divided into two parts: demand charge ($/kW) and energy consumption cost ($/kWh). It also has three different rate periods: off-peak, mid-peak and on-peak, and a summer and winter season [4].

This paper proposes two battery charging/discharging control methods for demand charge reduction during the on-peak rate period. Due to the dynamic nature of UCR's microgrid system, the MPC method is suitable because it involves a decision making process, at determined time intervals, yielding an optimized value that is fed back into the dynamic model [5].

II. INTRODUCTION TO THE MODEL OF THE REAL SYSTEM'S MPC ALGORITHM

The developed MPC algorithms consist of three main parts: 1) the predictive model; 2) the optimization model, and 3) the control law [6]. For the testing and validation of the two control methods, a sub-portion of the UCR microgrid is utilized consisting of 100 kW of solar PV, 500 kWh of battery energy storage system with a 100 kW battery inverter used to manage the flow of power in the 1200 CE-CERT research building.

A. Battery Energy Storage System Model

A 500 kWh Li-ion battery bank is installed in the testbed. To protect and prolong the lifetime of the Li-ion batteries in the microgrid, the SOC of the BESS is normally maintained between 40% and 90% [7]. In cases where solar generation is low, and the building energy consumption is high, the SOC is allowed to go down to 20%, for these special cases. From the charging and discharging experiments, the battery operation can be modeled as a linear process:

978-1-5090-2724-8/16/$31.00 ©2016 IEEE

$$\mathbf{bc}_L = \mathbf{bc}_{\mathbf{0}\,L} - \gamma \cdot \mathbf{A}_{L\times L} \cdot \mathbf{p}_L \tag{1}$$

where $\mathbf{bc}_L$ is the battery capacity vector; L is the entire battery operation time horizon.

$\mathbf{bc}_{\mathbf{0}\,L}$ is the initial battery capacity vector;

$\mathbf{A}_{L\times L} = \begin{bmatrix} 1 & 0 & \dots & 0 \\ 1 & 1 & \dots & 0 \\ \dots & \dots & \dots & \dots \\ 1 & 1 & \dots & 1 \end{bmatrix}_{L\times L}$ is a lower triangular matrix;

$\mathbf{p}_L$ is the battery operation vector;

γ is the charging/discharging efficiency.

B. Predictive Model

In the real system, both solar generation and building electricity usage should be predicted. For the given facility (1200 Building), the prediction model for solar generation and the building load profile are simplified by averaging the historical data.

$$\widehat{\mathbf{Ps}}_M = \frac{1}{n} \cdot \sum_{i=1}^{n} \mathbf{Ps}^i{}_M \tag{2}$$

$$\widehat{\mathbf{Pl}}_M = \frac{1}{n} \cdot \sum_{i=1}^{n} \mathbf{Pl}^i{}_M \tag{3}$$

where n represents for the amount of data samples chosen; M represents the amount of time intervals in the solar generation and building load model. The term $\mathbf{Ps}^i$, $\mathbf{Pl}^i$ represents the *i*-th data sample.

At any time interval *k*, the actual data for solar generation and building load is Ps_k and Pl_k ; $\widehat{\mathbf{Ps}}(k) / \widehat{\mathbf{Pl}}(k)$ is the k-th index of $\widehat{\mathbf{Ps}} / \widehat{\mathbf{Pl}}$.

For real-time solar generation Ps_k , if $\widehat{\mathbf{Ps}}(k) / Ps_k \geq \alpha$,

$$\widehat{\mathbf{Ps}}_k = \frac{Ps_k}{\widehat{\mathbf{Ps}}(k)} \cdot \widehat{\mathbf{Ps}} \ ;$$

$$\text{else } \widehat{\mathbf{Ps}}_k = \widehat{\mathbf{Ps}} .$$

For real-time building load Pl_k , if $Pl_k / \widehat{\mathbf{Pl}}(k) \geq \beta$,

$$\widehat{\mathbf{Pl}}_k (k : k + \Delta T) = \frac{\widehat{\mathbf{Pl}}(k)}{Pl_k} \cdot \widehat{\mathbf{Pl}}(k : k + \Delta T) ,$$

$$\widehat{\mathbf{Pl}}_k (k + \Delta T : M) = \widehat{\mathbf{Pl}}(k + \Delta T : M) ,$$

$$\text{else } \widehat{\mathbf{Pl}}_k = \widehat{\mathbf{Pl}} .$$

α , β are the fixed rate at which the solar generation and building load averaging profile should be updated in the real-time system, respectively. In our system, $\alpha = \beta = 1.2$. The building load profile is updated at some fixed portion since in the real system, high load only occurs for part of the entire on-peak rate period. In our system, $\Delta T = 2$ hours.

C. Optimization Model

As mentioned above, the TOU rate schedule includes two different cost components that should be considered in the optimization function. Therefore, the developed MPC control algorithms optimize for kWh and put a constraint to the kW demand to maintain it to the lowest value.

At each time slot:

$$\text{minimize } (\mathbf{price}_L^T)_k \cdot (\mathbf{pex}_L)_k \cdot \Delta t \tag{4}$$

$$\text{subject to } (\mathbf{bc}_L)_k = (\mathbf{bc}_{\mathbf{0}\,L})_k - \beta \cdot \Delta t \cdot A \cdot (\mathbf{p}_L)_k \tag{5}$$

$$0 \leq (\mathbf{pd}_L)_k \leq pda_k \cdot ONE \tag{6}$$

$$ONE \cdot disRate \leq (\mathbf{bc}_L)_k \leq bc_{\max} \cdot ONE \tag{7}$$

$$(\mathbf{pex}_L)_k = (\widehat{\mathbf{Pl}}_L)_k - (\widehat{\mathbf{Ps}}_L)_k + (\mathbf{pd}_L)_k \tag{8}$$

$$0 \leq (\mathbf{pex}_L)_k \leq onPeakini \cdot ONE \tag{9}$$

$(\mathbf{price}_L)_k$ represents the electricity price for time period $k : k + L - 1$;

$(\mathbf{pex}_L)_k$ represents the power from external grid/utility to the building;

$$pda_k = \frac{(bc_0)_k - disRate \cdot bc_{max}}{Remaining\ Time} \tag{10}$$

$$pdmax_k = \frac{(bc_0)_k - 0.2 \cdot bc_{max}}{Remaining\ Time} \tag{11}$$

represents the average discharging power at time *k*;

$ONE = \begin{bmatrix} 1 & \dots & 1 \end{bmatrix}_L^{\mathrm{T}}$;

disRate is the minimal SOC allowed to discharge;

onPeakini is the scheduled maximum value for the initial on-peak demand.

The battery operation vector is:

$$\mathbf{p}_{discharge} = \begin{bmatrix} (\mathbf{pd}_L)_1(1) \\ (\mathbf{pd}_L)_2(1) \\ \vdots \\ (\mathbf{pd}_L)_M(1) \end{bmatrix}$$

D. Constant Threshold MPC (CT-MPC) Algorithm

In our initial approach, the control algorithm is designed to always charge the BESS during the off-peak rate period and discharge during the on-peak rate period. For the control implementation, the duration for each time interval is 5 minutes which is chosen based on limitations posed by the net metering system. In this approach, the *onPeakini* in (9) is a constant value for the entire rate period, so it is called the constant threshold MPC (CT-MPC) algorithm. The CT-MPC algorithm principles can be described based on [8] at period *i*:

(i) At initial time $i = 0$, set optimization horizon M, where

$$M = \text{onpeak } hours \times 12 + 6.$$

As electricity demand charges are calculated based on a 15 minutes moving average by the utility company, the battery bank is programmed to start discharging 15 minutes prior to the on-peak rate period start time, and stop discharging 15 minutes past the end time. Therefore, 6 more time slots are added to the entire optimization horizon.

(ii) Set control horizon to 1 hour, which is $L = 12$ and fetch the prediction model $\widehat{\mathbf{Ps}}_{(M+L)}$ and $\widehat{\mathbf{Pl}}_{(M+L)}$. Additionally, fetch the electricity price $\mathbf{price}_{(\mathrm{M+L})}$ and set $disRate = 0.4$.

(iii) At time $i = k$, fetch the most updated system data: Ps_k, Pl_k, bc_k, bp_k, the electricity price $\mathbf{price}(k: k+L-1))_k$; update the prediction model $(\widehat{\mathbf{Ps}}(k: k+L-1))_k$ and $(\widehat{\mathbf{Pl}}(k: k+L-1))_k$

(iv) Calculate (10), (11). If $pda_k \le 0$, decrease *disRate* until $pda_k > 0$. Update *disRate*.

(v) When the building load is significantly large: $Pl_k - Ps_k - pda_k > onPeakini$

$$\mathbf{p}_{discharge}(i) = \begin{cases} pdmax_k, & Pl_k - Ps_k - onPeakini > pdmax_k \\ Pl_k - Ps_k - onPeakini \end{cases}$$

to make sure the minimal SOC is larger than 20% and maintain the lowest demand value.

(vi) Else, calculate optimization problem (4) with constraints (5) — (9). Obtain the result $(\mathbf{pd}_L)_k$ and only use the first index of $(\mathbf{pd}_L)_k$ to be the battery discharging operation: $\mathbf{p}_{discharge}(i) = (\mathbf{pd}_L)_k(1)$.

(vii) Set $i = k + 1$; then go back to step iv until $i = M$.

Under RPU's TOU rate schedule in the winter season, CT-MPC can control the BESS efficiently under stable building load and solar generation patterns

E. Adjusting Demand Threshold MPC (ADT-MPC) Algorithm

During the summer season, the on-peak rate period is from 12:00 to 18:00. Since the implemented microgrid system includes a research laboratory building, there are many experiments conducted with unpredictable equipment loads during working hours. Additionally, the influence of variable solar generation during the summer on-peak rate period is also increased due to more hours of overlap between solar generation and on-peak schedule. The forecast horizon of solar generation covers the entire on-peak rate period in the summer time which clearly increases the uncertainty of the solar generation prediction. The control law is to achieve appropriate demand threshold to compensate for a weaker forecast when the building load is high and/or solar generation is low.

To adjust to an appropriate value for *onPeakini*, ΔSOC (the deviation between actual change and predicted change) needs to be tracked among the control process. To track it, at time *k*, the $\Delta\mathbf{pd}_k$ vector is used to record the predicted discharging power at time slot $k+1$,

$$\Delta\mathbf{pd} = \begin{bmatrix} 0 \\ \Delta pd^1 \\ \dots \\ \Delta pd^{k-1} \end{bmatrix}_k$$

$$\Delta\mathbf{pd}(1) = 0,\ \Delta\mathbf{pd}(2) = \Delta pd^1,\ \dots,\ \Delta\mathbf{pd}(k) = \Delta pd^{k-1}$$

The control horizon changes from fixed L to descending $M - k + 1$. The detailed control principles are as follows:

(i) For each on-peak rate period of a day, time intervals can be divided into M, where hour is the hours of on-peak rate period in the summer, where $M = 78$.

(ii) At initial time, set time interval $i = 0$. Also, get the prediction model for solar generation and building load $\widehat{\mathbf{Ps}}_M$ and $\widehat{\mathbf{Pl}}_M$, respectively; get electricity price $\mathbf{price}_M$. Set $disRate = 0.4$, $\Delta SOC = 0$ and $onPeak = onPeakini$.

(iii) At time *k*, set optimization operation horizon $L_{des} = M - k + 1$; the updated prediction profiles for solar generation and the building load are changed to $(\widehat{\mathbf{Pl}}(k:M))_k, (\widehat{\mathbf{Ps}}(k:M))_k$.

(iv) Calculate the average discharging power from (10) and (11); when $pda_k \le 0$, decreases *disRate* until $pda_k > 0$. If pda_k or $pdamax_k$ is larger than 100, set them equal to 100 kW. Update *disRate*.

(v) If $Ps_k > Pl_k$, which means there is surplus solar energy generation,

$$\mathbf{pd}_{discharging}(k) = \begin{cases} Pl_k + 5 - Ps_k, Ps_k > Pl_k + 10 \text{ and } SOC < 90 \\ 0 \quad , \text{ else} \end{cases}$$

$$\Delta\mathbf{pd}(k) = pda_k$$

This is the particular charging process during the on-peak rate period.

(vi) If the optimization problem (4) with constraints (5) – (9) can be solved,

$$\Delta\mathbf{pd}(k) = \mathbf{pd}_k(2),$$

$$\mathbf{pd}_{discharge}(k) = \mathbf{pd}_k(1)$$

$$flag = flag + 1$$

flag means the continuously successful times of meeting the constraints

(vii) Else,

$$flag = 0$$

$$node = 1$$

$$\mathbf{p}_{discharge}(k) = \begin{cases} \min(Pl_k - Ps_k - \max(pex), size), & \Delta SOC > 0 \\ \min(Pl_k - Ps_k - onPeak), size), & \Delta SOC \le 0 \end{cases}$$

size is the variable for the system battery inverter which determines the maximum discharging/charging power. Here, $size = 100$.

(viii) Check $\mathbf{p}_{discharge}(k) \ge 0$, if not,

$$\mathbf{p}_{discharge}(k) = \begin{cases} 0 & , \quad SOC < 20 \\ Pl_k - Ps_k, & Pl_k - Ps_k < pda_k \\ pda_k & , \quad else \end{cases}$$

$$\Delta pd_{temp} = \begin{cases} \min(\widehat{\mathbf{Pl}}_k(2) - \widehat{\mathbf{Ps}}_k(2) - onPeak, 100), & \Delta SOC \le 0 \\ \min(\widehat{\mathbf{Pl}}_k(2) - \widehat{\mathbf{Ps}}_k(2) - \max(pex), 100), & \Delta SOC > 0 \end{cases}$$

$$\Delta \mathbf{pd}(k) = \begin{cases} pdamax_k & , \mathbf{pd}_{discharge}(k) > pdamax_k \\ pda_k & , \quad \Delta pd_{temp} > pda_k \\ \Delta pd_{temp} & , \quad else \end{cases}$$

If $\Delta \mathbf{pd}(k) < 0$, set $\Delta \mathbf{pd}(k) = pda$. Then, calculate

$$\Delta SOC_k = \sum_{i=t}^{k} \Delta SOC(i) = \begin{bmatrix} 1 & \cdots & 1 \end{bmatrix}_{(k-t+1)\times 1} \cdot (\mathbf{p}_{discharge}(t:k) - \Delta \mathbf{pd}(t:k)) \times \frac{\Delta t}{bc_{max}/100}$$

(ix) If $flag > 12$, set

$$onPeak = \max(onPeeakini, \max(pex))$$

(x) If $\Delta SOC_k \le \varepsilon$ and $node = 1$ or $\Delta SOC_k \le -5$,

$$onPeak = \max(\max(pex), onPeakini) - \frac{\frac{\Delta SOC}{100} \cdot bc_{max}}{k - t + 1}$$

t is the last time slot when these conditions were met;

ε is a factor for the time and range of the deviation to change *onPeak*. Smaller $|\varepsilon|$ results to quicker response time to change the threshold *onPeak*. In the below simulation, $\varepsilon = -3$.

For each new day in the month: check new maximum net load and set

$$onPeakini = \max(onPeakini, \max(pex))$$

III. Results and Comparison between CT-MPC Method and ADT-MPC Method

A. CT-MPC Algorithm Experiments

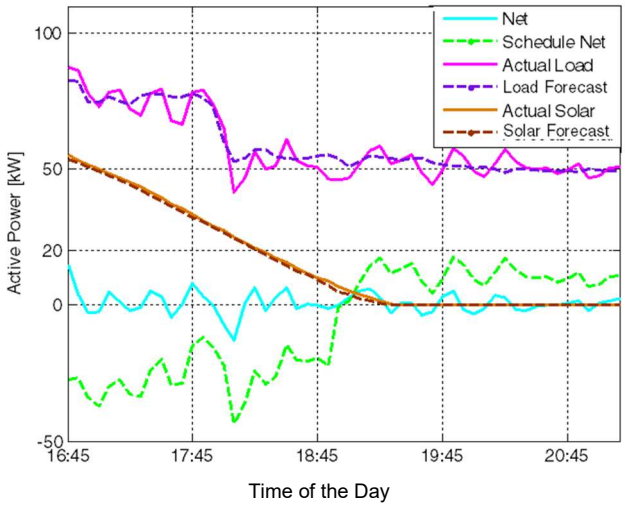

Fig.1. Solar Generation and Building Load Experiment.

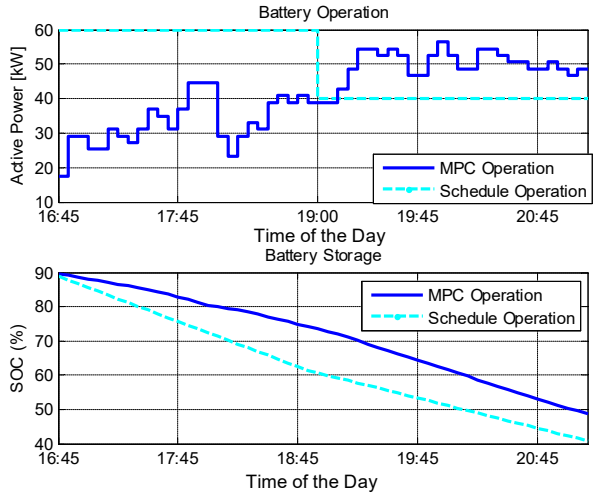

Fig.2. Battery Operation and SOC Level.

Figs 1 and 2 show a single-day experiment on 5/14/2015, under the winter season electrical rate schedule. The top panel in Fig. 2 shows that under 'Schedule Operation' the BESS was discharged at a fixed power for a certain period of time, without considering any system information.

In Fig.1, the *onPeakini* was set to 20 kW. It is clear to see that the net load was tightly controlled below *onPeakini* and most of the time it was around a zero net load value, which shows that no power needs to be supplied from the external grid. Alternately, under scheduled operation, the net load is always below 0 kW during the first two hours and around 20 kW during the last two hours. Although the scheduled operation can also

maintain the on-peak demand below *onPeakini*, a significant amount of energy produced by the SIGI microgrid was unnecessarily injected into the external grid. In Fig.2, the observed step-like trend of battery operation, is the result of the 5-minute time intervals that kept operation constant at a certain value. At the end of the on-peak rate period, the remaining SOC under CT-MPC Operation is 48.6%, while the SOC drops to 40% under scheduled operation. In Scenario 1, the MPC Operation can maximize the utilization of the battery capacity to achieve the minimum electricity consumption (kWh) and the on-peak demand (kW).

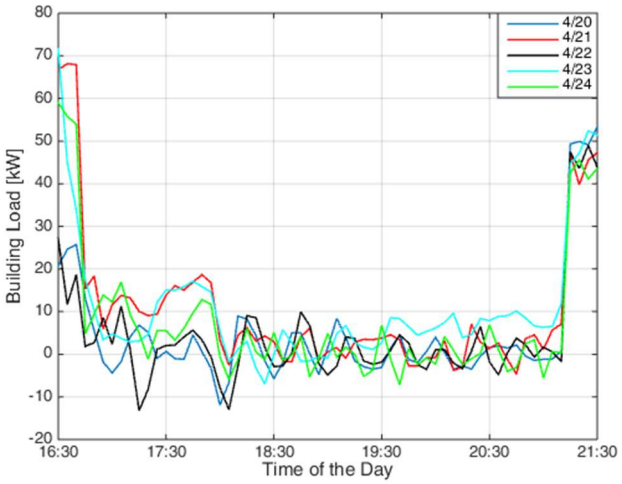

Fig.3. One-week Long Experiments Net Load Demonstration Under CT-MPC Algorithm.

In Fig.3, the net load for these days was tightly kept below *onPeakini* and most days the net was near zero. At 16:45/21:15 on each day, the BESS started/stopped discharging so the net load before/after was at a high level. With continuously experiments for different days, it is validated that the CT-MPC control algorithm presented in this work can control the BESS efficiently to maintain certain on-peak demand and the lowest power consumption in winter season. CT-MPC algorithm can meet the needs for demand load peak shaving applications.

In the winter season, the characteristics of solar generation and building load are relatively stable for most of the days and the forecast model can adjust well. Additionally, there are only 4 hours of the on-peak rate periods so the 250 kWh battery storage (40% --- 90% SOC) is capable to maintain a relatively low on-peak demand even with scheduled operation for most of the days. The CT-MPC algorithm utilizes the BESS in a more efficient and effective manner.

B. ADT-MPC Algorithm Simulation and Experiment

Figs 4 and 5 are generated under cloudy weather conditions. The solar and building load data for these two graphs are from 6/9/2015. The actual solar generation during this day is very low, which is much lower than the average solar generation profile. The actual building load profile of this day behaves randomly (increasing and decreasing throughout), which is at a high level compared to the average load profile.

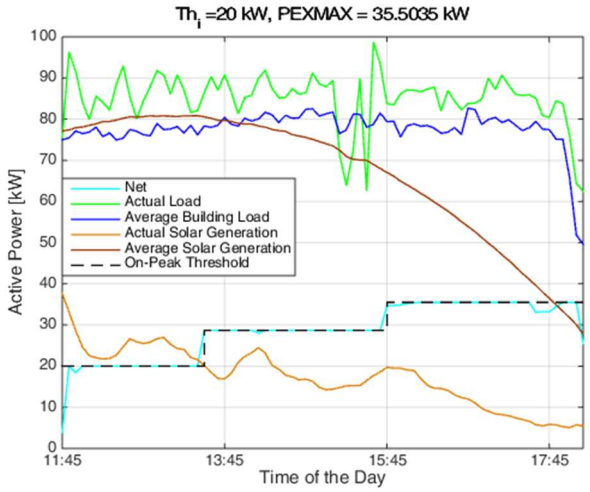

Fig. 4. ADT-MPC Net Load Simulation Under a Cloudy Day.

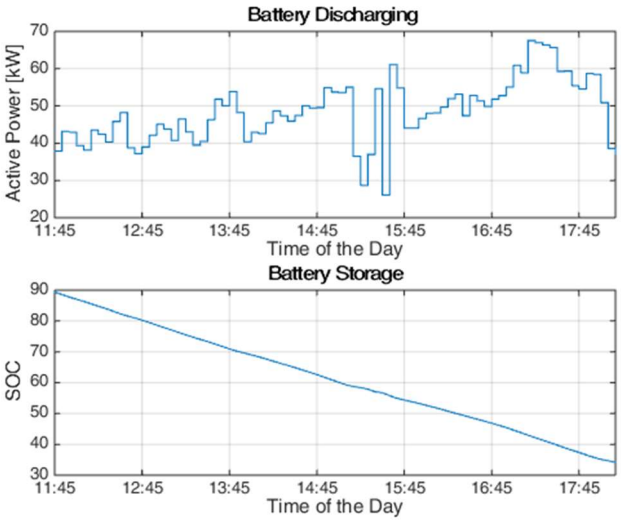

Fig.5. ADT-MPC Battery Operation and Storage Simulation Under a Cloudy Day.

Under these conditions, the battery should provide more energy to maintain a low on-peak demand value. From Fig.4 the on-peak threshold increases sequentially two times, from 20 kW to 35.5 kW at 14:05 ($i = 28$) and 15:45 ($i = 48$).

In Fig.5 the battery is discharged to 34.44% SOC which is still within the safety 20% SOC. Without the battery storage system, the maximum net load would have reached an on-peak demand value of 82.44 kW. With the help of the BESS contribution, the demand is decreased by 43.12 kW.

In the summer season (June to September), there is sufficient solar generation during most days of the months in Southern California. With the help of the BESS, the net load for most sunny days can be maintained near zero so the energy consumption from external grid is nearly zero during the on-peak rate period without adjusting the demand threshold. Due to the sufficient solar generation during on-peak period, there is surplus SOC left for using in the mid-peak rate period.

C. ADT-MPC and CT-MPC Simulation Comparison

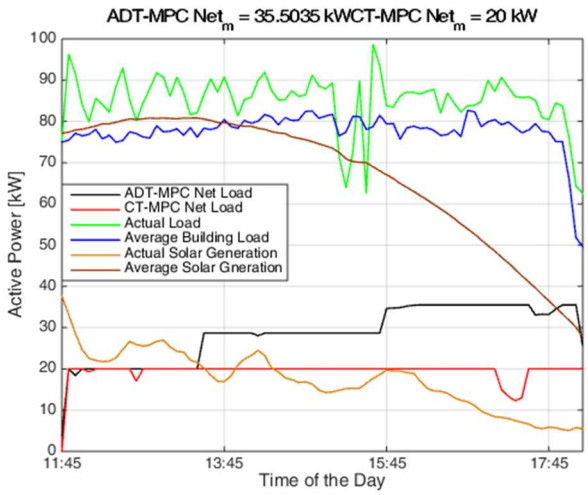

Fig.6. Net Load Comparison on a Cloudy Day.

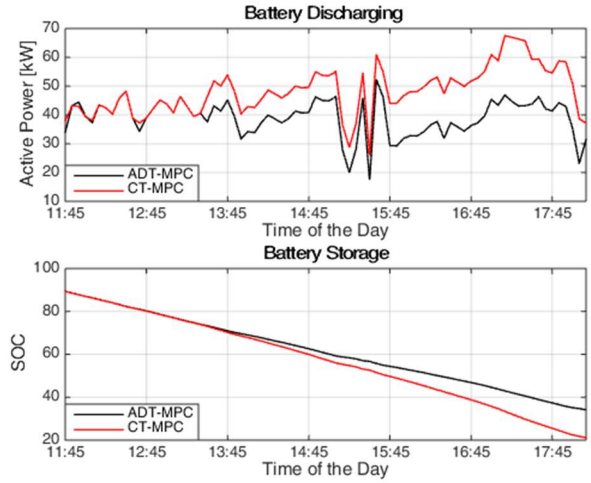

Fig.7. Battery Operation and Storage Comparison on a Cloudy Day.

Fig.6 shows the net load comparison between CT-MPC control algorithm and ADT-MPC control algorithm. The initial threshold is 20 kW. In this figure, it can be observed that the net load threshold has been adjusted to 39.32 kW under ADT-MPC operation while it is kept below 20 kW under CT-MPC operation. Initially, the first two hours of the battery operations are similar due to the similar demand threshold. After a couple of hours of operation, the threshold in the ADT-MPC algorithm is adjusted to a higher level due to the low solar generation. In Fig.7, the remaining SOC eventually decreases to 34% for ADT-MPC algorithm while it drops to the lowest level 20% in CT-MPC algorithm.

IV. Conclusion

From the comparison, it can be observed that CT-MPC will use the entire battery capacity to the lowest allowed SOC level (20%) to maintain the constant demand threshold, while the ADT-MPC algorithm adjusts the threshold to a higher value to maintain the battery capacity resulting in a higher SOC. The CT-MPC method was demonstrated to provide the lowest load demand resulting in lower battery SOC. The ADT-MPC algorithm maintains a higher SOC reserve capacity and is shown to be more responsive to demanding rate schedules and energy fluctuations. The CT-MPC performs well when coupled with accurate forecast models while the ADT-MPC algorithm excels when forecasting is more unpredictable. The ADT-MPC algorithm has the advantage of applicability to a highly variable system, when comprehensive historical energy generation or building load profiles are lacking.

References

[1] "MICROGRID DEFINITIONS," Microgrids at Berkeley Lab, [Online]. Available: https://building-microgrid.lbl.gov/microgrid-definitions. [Accessed 17 4 2016].

[2] U.S. Department of Energy's National Renewable Energy Laboratory (NREL)., "2014 Renewable Energy Data Book," 2015.

[3] "Solar Industry Data," Solar Energy Industries Association (SEIA), 2016. [Online]. Available: http://www.seia.org/research-resources/solar-industry-data. [Accessed 17 4 2016].

[4] City of Riverside Public Utilities Department, "Electric Schedule TOU- clean 2-1-2013," [Online]. Available: http://www.riversideca.gov/utilities/pdf/2013/Electric%20Schedule%20TOU-%20clean%202-1-2013.pdf. [Accessed 17 4 2016].

[5] R. Findeisen, F. Allgöwer and L. Biegler, Assessment and Future Directions of Nonlinear Model Predictive Control, Springer-Verlag Berlin Heidelberg, 2007.

[6] E. Camacho and C. Bordons, Model Predictive Control, London: Springer, 2007.

[7] "Thunder Sky Winston Energy Group Limited-WB-LYP1000AHC," Thunder Sky Winston Energy Group Limited, [Online]. Available: http://en.winston-battery.com/index.php/products/power-battery/item/wb-lyp1000ahc?category_id=176. [Accessed 17 4 2016].

[8] Y. Zhang, B. Liu, T. Zhant and B. Guo, "An Intelligent Control Strategy of Battery Energy Storage for Microgrid Energy Management under Forecast Uncertainties," *International Journal Of Electrochemical Science,* pp. 4190-4204, 2014.